Proceedings of the Thirty-fifth (2025) International Ocean and Polar Engineering Conference **www.isope.org**
Seoul/Goyang, Korea, June 1-6, 2025

ISBN 978-1-880653-74-6; ISSN 1098-6189

Numerical Calculations of Hydrodynamic Coefficient of SUBOFF Full Appendage Based on Overlapping Grid Method

Liang Li[1], Guohua Pan[2], Jianhua Wang[1], Decheng Wan[1]*

[1] Computational Marine Hydrodynamics Lab (CMHL), School of Naval Architecture, Ocean and Civil Engineering, Shanghai Jiao Tong University, Shanghai, China
[2] Ningbo Pilot Station, Ningbo Dagang Pilotage Co., Ltd., Ningbo, China

*Corresponding Author

ABSTRACT

In the development of modern marine technology, the hydrodynamic performance of submarine is very important to its maneuverability. However, under extreme maneuvering conditions, the complex dynamic behavior of submarines is difficult to accurately simulate by traditional experimental methods. In order to overcome the high cost and conditional limitations of experimental methods, numerical simulation technology came into being, providing an effective solution for this field. Based on the OpenFOAM overlapping grid method, the numerical simulation of the hydrodynamic coefficients of the SUBOFF full-attached submarine model is carried out. In the numerical calculation, the SST k-ω turbulence model is selected to simulate the moving viscous flow field. The hydrodynamic coefficients of submarines under two horizontal conditions of pure sway and pure yaw and two vertical conditions of pure heave and pure pitch are studied respectively. By fitting and calculating the hydrodynamic coefficients under four working conditions, compared with the experimental results, it can be seen that the hydrodynamic coefficients of sway and heave motion are well fitted. Among them, the fitting error of the inertial hydrodynamic coefficient is small, and most of the errors are within 30 %, while the error of the viscous hydrodynamic coefficient is large, and the vertical plane results are similar. The numerical simulation results are similar to the results of the current research field, which verifies the feasibility of calculating the hydrodynamic coefficient of the submarine based on the overlapping grid method and provides a reference for its hydrodynamic performance analysis.

KEYWORDS: SUBOFF; Overlapping grid; OpenFOAM; Hydrodynamic coefficient.

INTRODUCTION

Since ancient times, exploration of the ocean has never stopped in the human world. After entering the 21st century, with the continuous development of science and technology, various underwater vehicles have gradually become important tools in the fields of ocean exploration, resource exploitation, environmental monitoring and rescue, making people further develop and utilize the ocean. In the course of the development of underwater vehicles, submarines undoubtedly occupied an important position, from the 16th century Leonardo. Da Vinci first proposed the design of submarines to the advent of nuclear submarines in the 20th century. The research on the hydrodynamic performance of submarines by researchers around the world has deepened, and the maneuverability of submarines has been continuously improved. Among them, the study of various hydrodynamic coefficients is particularly important for submarines. Model test and numerical simulation are the two main research methods at present. Model test is mainly based on Planar motion mechanism (PMM) (Yang et al., 2009), which provides a large number of experimental data for studying the dynamic hydrodynamic performance of submarines. Because model tests require a lot of money and time, the use of numerical simulation technology to study the hydrodynamic coefficients of submarines provides an important solution in this field.

Scholars around the world have carried out a lot of academic research on the maneuverability of submarines and the numerical simulation of PMM tests. Mansoorzadeh et al. (2014) studied the hydrodynamic coefficient of autonomous underwater vehicle (AUV) by combining computational and experimental fluid dynamics methods. By constructing a dynamic mesh model for horizontal planar motion mechanism testing, Lin et al. (2022) provided a comprehensive hydrodynamic coefficient database for autonomous underwater vehicles from the perspective of numerical simulation and experimental verification. Pan et al. (2012) and Jeon et al. (2021) used Computational Fluid Dynamics (CFD) method to analyze the hydrodynamic characteristics of underwater objects under large angle motion through steady-state and unsteady-state simulation. The dynamic grid method was used to simulate maneuvering and compare with the experimental data to verify the accuracy of the simulation. At the same time, their maneuverability and dynamic behavior were evaluated. Suzuki et al. (2013) used CFD and 6DOF motion simulation to numerically simulate the two PMM motions of underwater vehicles and solved them by forced vibration test. The hydrodynamic coefficients obtained were compared with the experimental results to verify the accuracy of the numerical method. Lavrov et al. (2017) used the Navier-Stokes equations in OpenFOAM to simulate the flow near the 2D ship section under forced rolling motion and used the mixed Lagrangian-Eulerian adaptive mesh scheme to solve the forced motion and free surface capture problems. The hydrodynamic characteristics of container ships with different geometric characteristics and the influence of viscosity on vortex shedding and rolling motion were studied. Under the condition of ignoring the influence of free surface wave, Yang et al. (2011) simulated the pure swaying motion of KVLCC1 bare hull under the control of PMM in deep and shallow water and obtained its linear hydrodynamic coefficient. Liang et al. (2021) and Lin et al. (2018) conducted extensive and comprehensive PMM tests on the SUBOFF submarine model through model tests and numerical simulations and obtained a series of reliable hydrodynamic coefficients such as pure sway, pure yaw, pure heave, and pure pitch. Although numerical simulation can solve some flow problems, it may have some limitations for some more complex flow phenomena (such as separation, eddy current, etc.), and it consumes a lot of computing resources.

Based on the open source software OpenFOAM and overlapping grid technology, this paper takes the SUBOFF submarine model as the research object, and carries out four different motion forms of pure sway, pure yaw, pure pitch and pure heave under PMM control. Each motion form simulates five forced motions with different amplitudes and frequencies. Based on the unsteady RANS (Reynolds-Averaged Navier-Stokes) equation and SST (shear stress transport model) k-ω turbulence model, the viscous flow field of various motions is numerically simulated, and the hydrodynamic coefficients of SUBOFF under various working conditions are numerically fitted. Through numerical simulation and fitting results, this paper provides a detailed analysis of the hydrodynamic characteristics of SUBOFF under different motion conditions and provides a new numerical simulation method and reference for submarine design and performance optimization as well as greatly saves the cost of computing resources.

NUMERICAL METHOD

Governing Equation

The SUBOFF submarine model numerically simulates the motion under PMM control based on the incompressible RANS equation. The equation is as follows :

$$\begin{cases} \nabla \cdot \mathbf{U} = 0 \\ \dfrac{\partial \rho \mathbf{U}}{\partial t} + \nabla \cdot (\rho(\mathbf{U} - \mathbf{U}_g)\mathbf{U}) = \\ -\nabla p_d - \nabla \cdot (\rho \cdot \mathbf{g} \cdot \mathbf{x}) + \nabla \cdot (\mu_{eff} \nabla \mathbf{U}) + (\nabla \mathbf{U}) \cdot \nabla \mu_{eff} \end{cases} \tag{1}$$

The meaning of each parameter in the formula is as follows : $\mathbf{U}$ is the velocity field ; $\mathbf{U}_g$ is the grid moving speed ; t is time ; $P_d = P - \rho.\mathbf{g}.\mathbf{x}$ is the hydrodynamic pressure ; ρ is the liquid density ; $\mathbf{g}$ is the acceleration vector of gravity ; $\mu_{eff} = \rho\ (\ v + v_t)$ is the effective dynamic viscosity, v and v_t are the dynamic viscosity and turbulent eddy viscosity, and the latter is solved by the turbulence model.

Turbulent Flow Model

The SST (shear stress transport model) k-ω turbulence model significantly improves the simulation accuracy of complex flows by combining the high accuracy of the k-ω model in the near-wall region and the stability of the k-ε model in free flow, as well as the limitation of mixing function and turbulent viscosity. Therefore, the SST k-ω turbulence model is used to solve the turbulent eddy viscosity v_t in Eq. 2. The equation is:

$$\begin{cases} \dfrac{\partial k}{\partial t} + \nabla \cdot (\mathbf{U}k) = \tilde{G} - \beta^* k\omega + \nabla \cdot \left[(v + \alpha_k v_t) \nabla k \right] \\ \dfrac{\partial \omega}{\partial t} + \nabla \cdot (\mathbf{U}\omega) = \\ \gamma S^2 - \beta\omega^2 + \nabla \cdot \left[(v + \alpha_\omega v_t) \nabla \omega \right] + (1 - F_1) CD_{k\omega} \end{cases} \tag{2}$$

The meaning of each parameter in the formula is as follows : k is turbulent kinetic energy ; ω is the turbulent dissipation rate ; t is time ; β and β^* are limiting factors ; α_k and α_ω are modified dynamic viscosity coefficients ; γ is the time percentage of turbulent fluctuation in the boundary layer ; F_1 is a mixed function, where the F_1 function can realize the switching between the near-wall standard k-ω model and the far-field standard k-ε model. The equation is:

$$F_1 = \tanh\left\{ \left\{ \min\left[\max\left(\frac{\sqrt{k}}{\beta^* \omega y}, \frac{500v}{y^2\omega} \right), \frac{4\alpha_{\omega_2} k}{CD^*_{k\omega} y^2} \right] \right\}^4 \right\} \tag{3}$$

where y is the distance to the nearest wall; ω_2 is a constant with a value of 0.856; the definitions of $CD_{k\omega}$ in Eq. 2 and $CD^*_{k\omega}$ Eq. 3 can be expressed as:

$$\begin{cases} CD_{k\omega} = 2a_{\omega 2} \nabla k \cdot \dfrac{\nabla \omega}{\omega} \\ CD^*_{k\omega} = \max\left(CD_{k\omega}, 10^{-10} \right) \end{cases} \tag{4}$$

For Eq. 2, $\tilde{G}$ is defined as follows:

$$\tilde{G} = \min\left\{ G, c_1 \beta^* k\omega \right\} \tag{5}$$

In the formula, c_1 is a constant and the value is 10; G is defined as follows:

$$G = v_t S^2 \tag{6}$$

In the formula, S represents the invariant of strain rate, which is obtained by the strain rate tensor in the standard k-ω model. The equation is:

$$\begin{cases} S_{ij} = \dfrac{1}{2}\left(\nabla \mathbf{U} + \nabla \mathbf{U}^T \right) v_t S^2 \\ S = 2\sqrt{2 S_{ij} S_{ij}} \end{cases} \tag{7}$$

The turbulent eddy viscosity v_t is obtained by Eq. 8, where a_1 is a constant and the value is 0.31. F_2 is a mixed function, and its definition is shown in Eq. 9.

$$v_t = \frac{a_1 k}{\max(a_1\omega, SF_2)} \tag{8}$$

$$F_2 = \tanh\left\{\left[\min\left(\frac{2\sqrt{k}}{\beta^*\omega y}, \frac{500v}{y^2\omega}\right)\right]^2\right\} \tag{9}$$

GEOMETRY AND WORKING CONDITION DESIGN

Geometric Model

In order to study the hydrodynamic coefficients of submarines, this paper selects the SOBOFF fully-attached submarine model specially designed by the US Defense Advanced Technology Research Agency DARPA for the establishment of submarine CFD analysis software database. The main body of the model consists of a hull, a command platform and four tail rudder wings symmetrically distributed in a cross shape. The total length is 104.5m. The plane motion under the control of four PMMs is numerically simulated with a scale ratio of 1:24. The geometric model and main scale are shown in Fig.1 and Table 1. The coordinate system adopts two right-handed rectangular coordinate systems, which are the geodetic coordinate system fixed on the earth and the body coordinate system fixed on the hull. The geodetic coordinate system is used to determine the spatial position and direction, and the body coordinate system is used to determine the hydrodynamic load and torque of the submarine. The geodetic coordinate system takes the front end of the bow as the origin coordinate, the *x*-axis points to the stern of the boat as the positive, the *y*-axis points to the starboard as the positive, the *z*-axis is positive, and the origin of the body coordinate system is located at the center of gravity of the submarine.

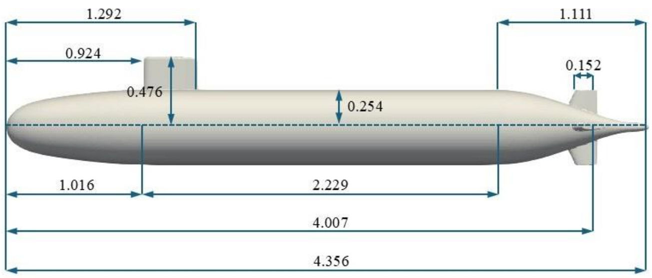

Fig. 1 SUBOFF full-attachment geometric model

Table 1. Main scale of model

Main dimensions	Value
Scale ratio	24
Forebody L_f /m	1.016
Raft body L_m /m	2.229
Afterbody L_f /m	1.111
Overall length L /m	4.356
Middle rotary diameter D /m	0.508
Vertical barycentric coordinates x_G /m	2.010
Horizontal barycentric coordinates y_G /m	0.001
Vertical barycentric coordinates z_G /m	0.0022

Mathematical Model Of Motion

By establishing the horizontal motion equation suitable for CFD calculation under PMM control, the corresponding hydrodynamic coefficient calculation formula is obtained. Because the derivation process of pure sway, pure yaw, pure heave and pure pitch is similar, only the derivation process of pure sway is introduced. The main motion parameters are as follows:

$$\begin{cases} \eta = a\sin\omega t \\ \varphi = \dot{\varphi} = 0 \\ V = \dot{\eta} = a\omega\cos\omega t \\ \dot{V} = -a\omega^2\sin\omega t \end{cases} \tag{10}$$

The meaning of each parameter in the formula is as follows: η is the lateral displacement; a is amplitude; ω is the frequency; t is time; φ is the speed of yaw; $\dot{\varphi}$ is the first-order coefficient of φ; V is the transverse velocity; $\dot{V}$ is the lateral acceleration. The motion is simplified, and the motion equation is as follows:

$$\begin{cases} Y = Y_0 + Y_{\dot{V}}\dot{V} + Y_V V \\ N = N_0 + N_{\dot{V}}\dot{V} + N_V V \end{cases} \tag{11}$$

In the formula, Y_0 and N_0 are constant terms of the initial state, and the value is 0, which can be omitted. The four terms of $Y_{\dot{V}}\dot{V}$, $Y_V V$, $N_{\dot{V}}\dot{V}$, $N_V V$ are the hydrodynamic coefficient; V is the velocity, $\dot{V}$ is the acceleration, Y is the lateral force, N is the yaw moment. The motion parameters are brought into Eq. 11 and the dimensionless processing is carried out. The motion equation is:

$$\begin{cases} Y = -\frac{1}{2}\rho L^3 Y'_{\dot{V}} a\omega^2\sin\omega t + \frac{1}{2}\rho U L^2 Y'_V a\omega\cos\omega t \\ N = -\frac{1}{2}\rho L^4 N'_{\dot{V}} a\omega^2\sin\omega t + \frac{1}{2}\rho U L^3 N'_V a\omega\cos\omega t \end{cases} \tag{12}$$

In the formula, U is the linear velocity; L is the captain; ρ is density. Therefore, the dimensionless hydrodynamic coefficient is:

$$Y'_{\dot{V}} = \frac{Y_{\dot{V}}}{\frac{1}{2}\rho L^3}, N'_{\dot{V}} = \frac{N_{\dot{V}}}{\frac{1}{2}\rho L^4}, Y'_V = \frac{Y_V}{\frac{1}{2}\rho U L^2}, N'_V = \frac{N'_V}{\frac{1}{2}\rho U L^3} \tag{13}$$

In the formula, $Y'_{\dot{V}}$ and Y'_V are dimensionless hydrodynamic coefficients of lateral force; $N'_{\dot{V}}$ and N'_V are dimensionless hydrodynamic coefficients of turning moment. Through the numerical simulation results of multiple working conditions, the curve fitting of the lateral force and the turning moment is carried out to obtain the fitting form of the motion equation, so as to obtain the dimensionless hydrodynamic coefficient. The equation is as follows:

$$\begin{cases} Y' = A\sin\omega t + B\cos\omega t \\ N' = C\sin\omega t + D\cos\omega t \end{cases} \tag{14}$$

where A and B are $Y'_{\dot{V}}$ and Y'_V; C and D are $N'_{\dot{V}}$ and N'_V.

Similarly, the hydrodynamic coefficient of pure heave can be obtained, which corresponds to the pure sway, which are $Z_{\dot{W}}$ 、 $M_{\dot{W}}$ 、 Z_W 、 M_W, respectively. The hydrodynamic coefficients of pure yaw are $Y_{\dot{r}}$ 、 $N_{\dot{r}}$ 、

Y_r 、 N_r ; hydrodynamic coefficient of pure pitch $Z_{\dot{q}}$、$M_{\dot{q}}$、Z_q 、M_q. Therefore, the dimensionless hydrodynamic coefficients can be obtained as $Z'_{\dot{W}}$ 、 $M'_{\dot{W}}$ 、 Z'_W 、 M'_W、 $Y'_{\dot{r}}$ 、 $N'_{\dot{r}}$ 、 Y'_r 、 N'_r 、 $Z'_{\dot{q}}$、 $M'_{\dot{q}}$、 Z'_q 、 M'_q.

Computational Domain Setting and Grid Independence

By using the dynamic overlapping grid technology, the numerical simulation of SUBOFF multiple motions under the control of PMM is carried out. The grid setting is mainly composed of two parts, namely the overlapping grid area and the background grid area. Because the motion attitude of the submarine is different when it moves in the horizontal plane and in the vertical plane, the computational domain is larger. Fig.2 shows the setting of the computational domain. Among them, the background grid area range is : $-1.15L < x < 3.45L$, $-1.15L < y < 1.15L$, $-1.15L < z < 1.15L$; the overlapping grid area is smaller than the background grid area, and the range is : $-0.46L < x < 1.46L$, $-0.46L < y < 0.46L$, $-0.46L < z < 0.46L$. The boundary conditions are established based on the principles of incompressible flow conservation and kinematic constraints. The boundary conditions are defined in accordance with the conservation laws of incompressible flow and kinematic constraints. The inlet velocity is specified using the fixedValue condition to ensure mass conservation, while the pressure is set with the zeroGradient condition to maintain the self-consistency of the pressure field. At the outlet, the inletOutlet condition is applied to the velocity to suppress backflow oscillations, with the pressure also set to zeroGradient to satisfy the Poisson equation. On the SUBOFF surface, the movingWallVelocity condition is used to impose a non-slip boundary, and zeroGradient pressure is applied to ensure the momentum balance at the wall. Additionally, the symmetryPlane condition is implemented on the bottom, ymax, and ymin surfaces, effectively reducing the size of the computational domain through mirror constraints.

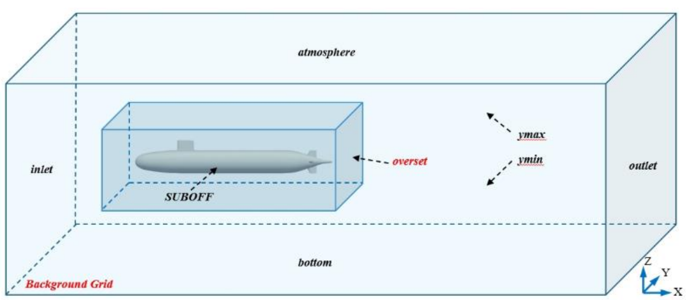

Fig. 2 Working condition diagram

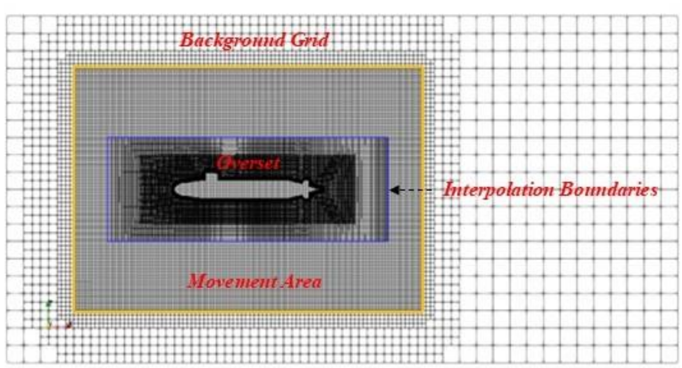

Fig. 3 Grid division

The snappyHexMesh tool provided by OpenFOAM is used for the orthogonal meshing, and the meshing diagram is shown in Fig. 3. Among them, the inner area of the blue frame is the overlapping grid area, and the outer area is the background grid area. In order to ensure the accuracy of the calculation results, the grid size at the transition from the overlapping grid area to the background grid area should be basically the same. Therefore, the background grid is refined three times to achieve the same size as the outermost grid size of the overlapping grid. The blue line is the interpolation boundary between the two parts of the grid. The grid range between the yellow line and the blue line is the motion area under the control of PMM.

For the surface boundary layer of the SUBOFF model, the isometric sequence division strategy (the first layer thickness 0.00376 m, 5 layers, growth rate 1.2) is adopted, and the background domain and the overlapping domain are divided into three-dimensional uniform grids. Due to the numerical flow field simulation of SUBOFF's four PMM motions in the horizontal and vertical planes, it is necessary to consider the x, y and z directions when verifying the grid convergence. The number of grids in the three directions increases by a ratio of $\sqrt[3]{2}$, and three sets of systematic grid systems of 2.35 million (Coarse), 4.41 million (Medium), and 8.6 million (Fine) were constructed.

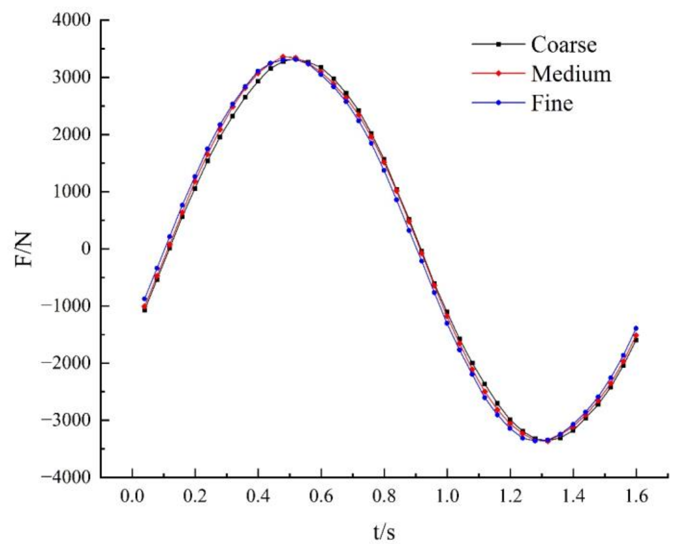

Fig. 4 Time history curve of swaying force for three grid sets

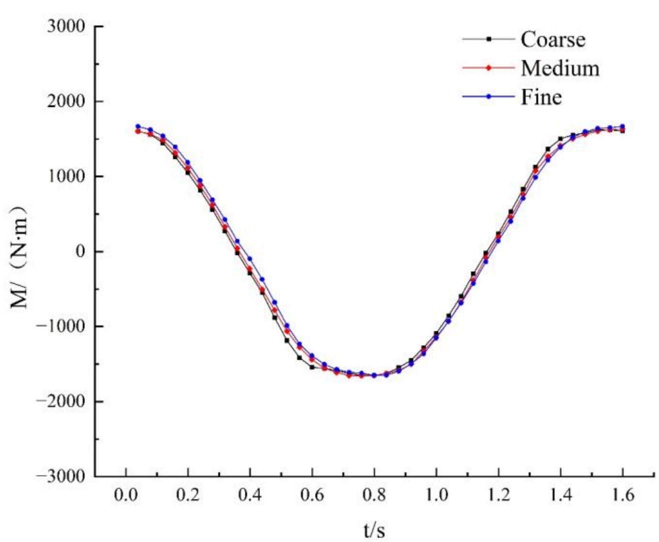

Fig. 5 Time history curve of yaw moment for three grid sets

To assess the impact of grid resolution on flow field results during SUBOFF's PMM motion in a complex flow field, convergence verification is performed using unidirectional flow. Simulations are conducted for SUBOFF in pure sway motion with an amplitude of 0.3 m, frequency of 0.625 Hz, and flow velocity of 3 m/s. Three grid resolutions are tested: 2.35 million, 4.41 million, and 8.6 million cells. A calculation time of 6.4 s is used to ensure full development of the flow field.

As illustrated in Fig.4 and Fig.5, numerical investigations on the SUBOFF model's pure sway motion demonstrate grid-converged hydrodynamic characteristics. Comparative analysis of three grid resolutions (Coarse, Medium, Fine) reveals consistent periodic sway force and yaw moment modes patterns during the post-flow-stabilization phase (fourth cycle, 1.6s window). The force amplitudes exhibit minimal sensitivity to grid refinement, measuring 3,312 N (Coarse), 3,359 N (Medium), and 3,342 N (Fine) with <1.5% inter-grid variation. Grid independence verification confirms the medium-resolution configuration (4.41M elements: 2.28M background + 2.13M overlapping grids) as optimal for PMM experiments, achieving computational economy without compromising hydrodynamic fidelity.

CALCULATION CONDITION SETTING

The SST k-ω turbulence model is used to simulate the various motions under the control of PMM. The same working conditions as the model scale test carried out by the David Taylar Experimental Center of the United States are adopted. The flow velocity is 3 m/s to simulate the speed of the submarine. The total calculation time is set to 5 cycles, and the time step is 0.001 seconds, which accelerates the calculation efficiency.

For pure sway and pure heave motion, the working conditions are similar and are designed using the control variable method, as shown in Table 2. Similarly, for pure yaw and pure pitch motion, the conditions are comparable. In terms of pure yaw motion, its motion is achieved by changing the yaw angle at the same speed and is accompanied by lateral displacement. In the numerical calculation, the motion is completed by the superposition of the lateral and yaw motions. The two frequencies are the same, and the phase difference is 1 / 4 period, both of which are sinusoidal motions. Among them, the lateral displacement of the pure yaw motion can be derived from the motion process of the underwater vehicle, and the maximum rotation angle ψ_0 = 10 °. The working conditions are set as shown in Table 3.

Table 2. Pure sway and pure heave condition setting

Operating conditions	a /m	f/Hz	T/s	ω/(rad/s)
1	0.3	0.2	5	1.2566
2	0.3	0.25	4	1.5708
3	0.3	0.3125	3.2	1.9635
4	0.3	0.4	2.5	2.5133
5	0.3	0.5	2	3.1416
6	0.3	0.625	1.6	3.9270

Table 3. Pure yaw and pure pitch condition settings

Operating conditions	a /m	f/Hz	T/s	ω/(rad/s)
1	0.4167	0.2	5	1.2566
2	0.3333	0.25	4	1.5708
3	0.2667	0.3125	3.2	1.9635
4	0.2083	0.4	2.5	2.5133
5	0.1666	0.5	2	3.1416
6	0.1333	0.625	1.6	3.9270

RESULT ANALYSIS

Aiming at the plane motion of SUBOFF under the control of four kinds of PMM, this study will discuss in detail from two aspects. The first aspect analyzes the submarine's motion characteristics through flow field results, while the second explores the impact of different control modes on the dynamic response via numerical fitting of hydrodynamic coefficients. These analyses aim to comprehensively assess the effect of PMM control on submarine plane motion performance and provide a theoretical foundation for submarine design and operation.

Flow Field Analysis

For the results of four kinds of motion flow fields at different frequencies, because the flow field results of pure sway and pure heave, pure yaw and pure pitch are similar, we only analyze the velocity field and pressure field of pure sway and pure yaw at different frequencies and take f = 0.2 Hz and f = 0.625 Hz to analyze their motion in the fifth calculation cycle. For pure sway motion, only the velocity and pressure fields at the maximum amplitude are considered, as shown in Fig. 6. For pure yaw, both the flow field results at the maximum motion amplitude and maximum rotation angle are included, as shown in Fig. 7.

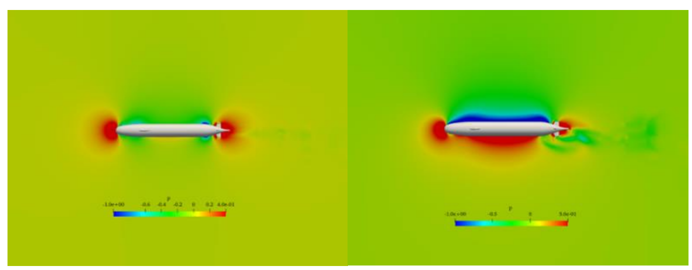

(a) When t = 0.25 T, f = 0.2 Hz and f = 0.625 Hz, the pressure cloud diagram is shown.

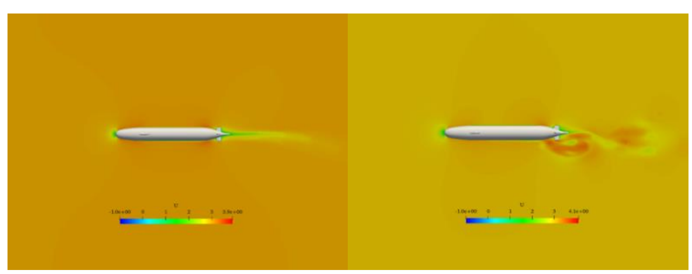

(b) When t = 0.25 T, f = 0.2 Hz and f = 0.625 Hz, the velocity cloud diagram is shown.

Fig. 6 Results of the maximum amplitude flow field of pure swaying motion

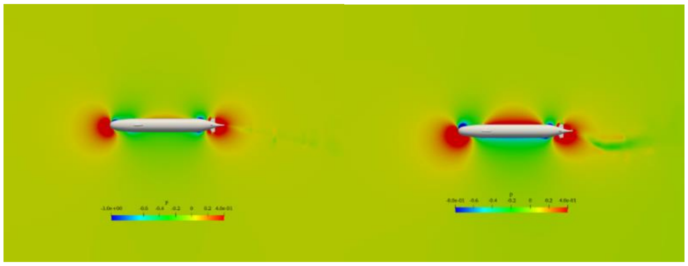

(a) When t = 0.25 T, f = 0.2 Hz and f = 0.625 Hz, the pressure cloud diagram is shown.

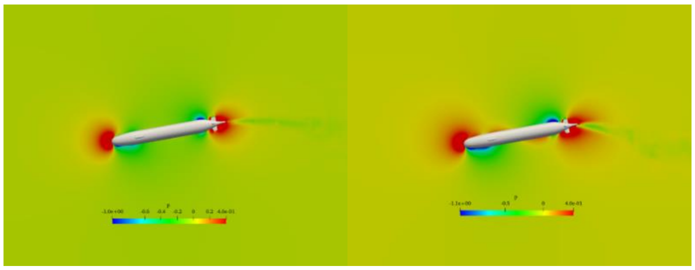

(b) When t = 0.5 T, f = 0.2 Hz and f = 0.625 Hz, the pressure cloud diagram is shown.

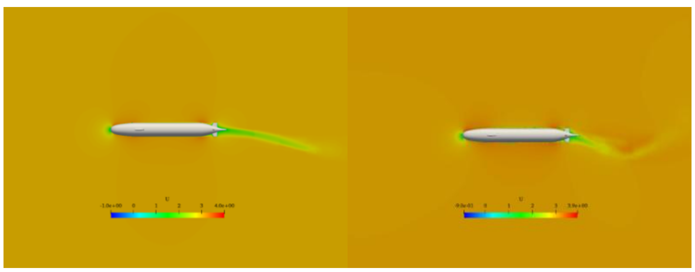

(c) When t = 0.25 T, f = 0.2 Hz and f = 0.625 Hz, the velocity cloud diagram is shown.

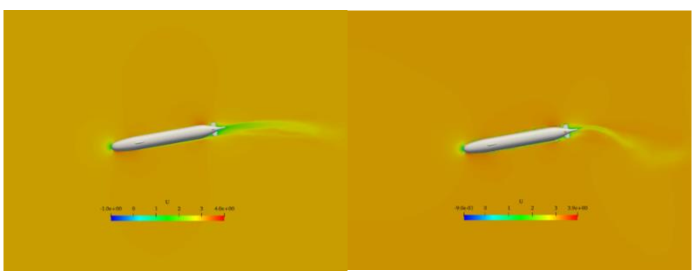

(d) When t = 0.5 T, f = 0.2 Hz and f = 0.625 Hz, the velocity cloud diagram is shown.

Fig. 7 The flow field results at the maximum amplitude of pure yaw motion and the maximum amplitude of rotation angle (The motion amplitudes of a and c are the largest, and the rotation amplitudes of b and d are the largest)

Fig. 6 shows that at t = 0.25T, the SUBOFF submarine reaches maximum sway amplitude. At f = 0.2 Hz, the lateral displacement velocity is slower than at f = 0.625 Hz, with a relatively stable flow field, regular velocity distribution, and dispersed vortex structure. However, both inflow and outflow sections exhibit some speed jump. The flow disturbance is mainly concentrated on the submarine's sides, and the pressure field remains more uniform with a small gradient. At f = 0.625 Hz, the increased motion frequency significantly alters the flow field, intensifying vortex formation and flow irregularity, while the flow velocity increases. The pressure field exhibits noticeable fluctuations, especially on the submarine's sides, with an increased pressure gradient and pronounced fluid separation and backflow.

Fig. 7 shows that SUBOFF undergoes pure yaw motion, with t = 0.25T and t =0.5T corresponding to the maximum motion and angle amplitudes, respectively. At f = 0.2 Hz, the submarine bow moves slowly, with gentle fluid motion, a symmetrical velocity field, a uniform pressure distribution, and minimal fluid separation. At f = 0.625 Hz, increased inertia amplifies the submarine's motion, intensifying flow disturbances and promoting vortex formation. This causes noticeable pressure fluctuations at the bow and stern, with a large pressure gradient, especially at the bow, where flow separation leads to local pressure increases and flow instability.

Comparing the flow field changes at different frequencies reveals that motion frequency significantly affects water flow disturbance. High-frequency motion causes more intense changes in the flow and pressure fields, leading to a more complex flow structure and greater hydrodynamic effects. These changes are crucial for the hydrodynamic design and motion control of submarines.

Hydrodynamic Coefficient Analysis

By analyzing the hydrodynamic numerical calculation results of SUBOFF submarine under different PMM motion modes, the values of A, B, C and D under four kinds of motion are obtained, and the hydrodynamic coefficients related to various PMM motions are obtained by linear fitting. Fig.8, Fig.9, Fig.10 and Fig.11 represent the hydrodynamic coefficient fitting curves of pure sway, pure heave, pure yaw and pure pitch respectively.

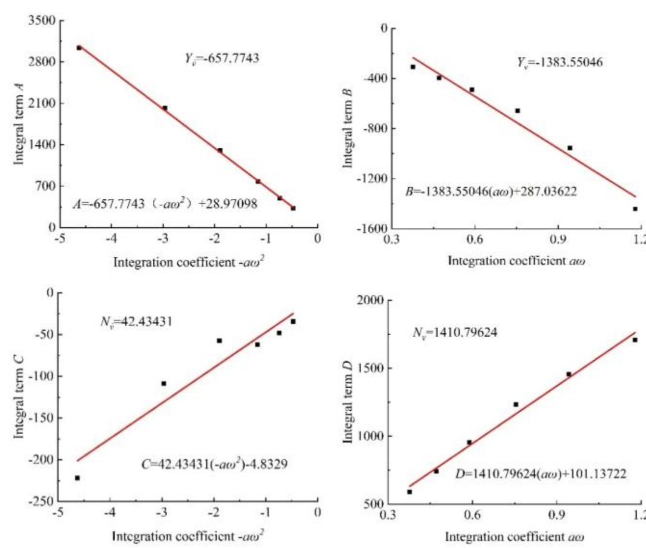

Fig. 8 Pure sway hydrodynamic coefficient fitting curve

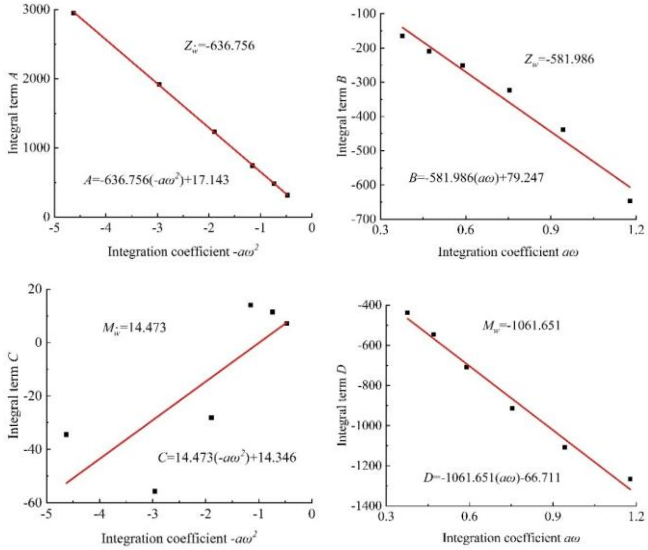

Fig. 9 Pure heave hydrodynamic coefficient fitting curve

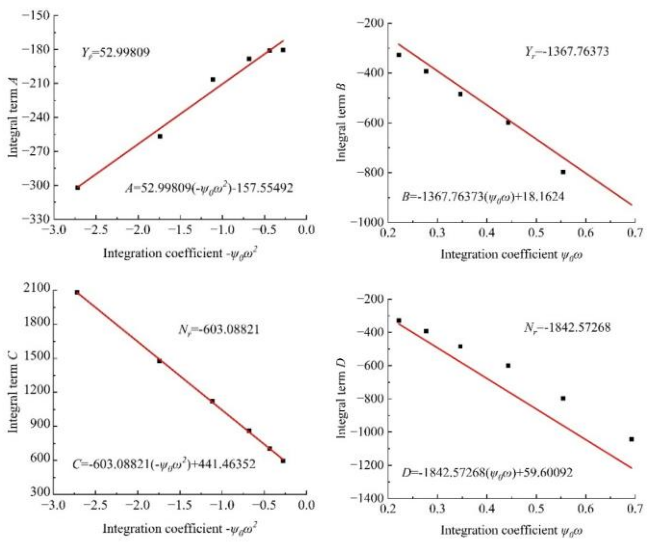

Fig. 10 Pure yaw hydrodynamic coefficient fitting curve

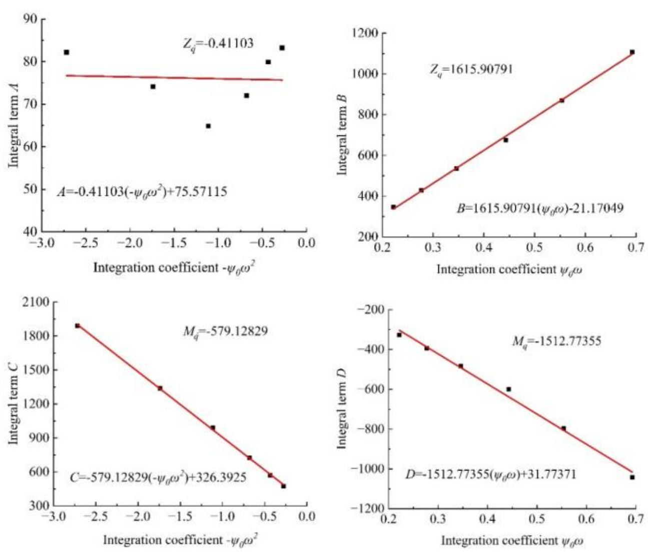

Fig. 11 Pure pitch hydrodynamic coefficient fitting curve

By dimensionless processing of various hydrodynamic coefficients obtained by fitting and comparing with the hydrodynamic data published in the SUBOFF full-attachment maneuverability test done by the Taylor Research Center of the United States (Roddy, 1990), the first 8 items in the table are inertial hydrodynamic coefficients, and the last 8 items are viscous hydrodynamic coefficients. The calculation results are shown in table 4.

Table 4. Non-dimensional hydrodynamic coefficient calculation results

Dimensionless hydrodynamic coefficients	*Numerical simulation values*	Test values	Absolute value of error/%
$Y'_{\dot v}$	-0.0165901	-0.016191	2.47
$N'_{\dot v}$	0.0002511	0.000396	36.57
$Z'_{\dot w}$	-0.0154078	-0.014529	6.05
$M'_{\dot w}$	0.0000804	-0.000561	114.26
$Y'_{\dot r}$	0.0002944	0.000398	26.03
$N'_{\dot r}$	-0.0007691	-0.000897	14.27
$Z'_{\dot q}$	-0.0000023	-0.000633	100.36
$M'_{\dot q}$	-0.0007385	-0.000861	14.13
Y'_V	-0.0495629	-0.027830	78.08
N'_V	0.0001186	-0.013650	100.86
Z'_W	-0.0204478	-0.013910	47.84
M'_W	-0.0085630	0.010324	179.61
Y'_r	-0.0110320	0.005250	309.52
N'_r	-0.0034118	-0.004440	23.16
Z'_q	0.0130335	-0.007550	272.18
M'_q	-0.0028011	-0.003700	24.32

From the calculation results in Table 4, it can be seen that the dimensionless hydrodynamic coefficients obtained by fitting the SUBOFF submarine model under the control of PMM as a whole, the inertial hydrodynamic coefficients are in good agreement with the experimental results of the Taylor Research Center in the United States, while the viscous hydrodynamic coefficients have large errors, especially in the angular velocity coefficients related to pure yaw and pure pitch. There is a significant deviation between the calculation results and the experimental data. From the perspective of numerical simulation, this error is mainly due to the poor simulation accuracy of the separated flow in the simulation of submarine PMM motion by the currently used SST *k-ω* turbulence model. In addition, the mathematical model used in PMM motion is based on the assumption of small amplitude linearity, and the interaction between nonlinear terms and coupling effects is not considered, which is also one of the important reasons for the error. It should be pointed out that the large error of viscous hydrodynamic coefficient is a common problem in this field.

By calculating the hydrodynamic coefficients, the Matlab-based underwater vehicle rotation trajectory prediction module is employed for numerical simulations to determine the tactical diameter, positive transverse distance, and advance distance of the SUBOFF model. The results are found to exhibit a small error when compared with those derived from hydrodynamic coefficients in existing literature. This discrepancy may be attributed to the relatively limited influence of viscous hydrodynamic coefficients on the maneuverability predictions of underwater vehicles.

CONCLUSIONS

In this study, the open-source software OpenFOAM is employed, and the SUBOFF submarine is chosen as the research object using the overlapping grid method. The unsteady Reynolds-averaged Navier-Stokes (RANS) equations, coupled with the SST k-ω turbulence model, are used to simulate the four motions—pure sway, pure heave, pure yaw, and pure pitch—under the control of the Planar Motion Mechanism (PMM). The flow field results for each motion, along with various hydrodynamic coefficients obtained through numerical fitting, are thoroughly analyzed. Regarding the flow field results, the vertical plane exhibits similar characteristics to the horizontal plane. Under low-frequency conditions (f = 0.2 Hz), both the pure sway and pure yaw motions of the SUBOFF submarine generate relatively stable flow fields, where the vortex structures are dispersed and the pressure field remains uniform. In contrast, under high-frequency conditions (f = 0.625 Hz), as the submarine's motion frequency increases, significant changes in both the flow field and pressure field occur. The vortex and flow irregularity intensify, pressure fluctuations become more pronounced, and fluid separation is enhanced; In terms of various hydrodynamic coefficients obtained by fitting, the error of inertial hydrodynamic coefficients is small, and the error of viscous hydrodynamic coefficients is large, especially in the angular velocity coefficients. The reason for the analysis error may be due to the insufficient accuracy of the turbulence model to simulate the separation flow and the PMM motion mathematical model. The interaction between the nonlinear term and the coupling term is not considered, but this is similar to the calculation results in the current field. Through the analysis of the above calculation results, it can be seen that it is feasible to use the overlapping grid method to calculate the hydrodynamic coefficient of the submarine. The maneuverability index obtained by numerical simulation through the Matlab underwater vehicle rotation trajectory prediction module is compared with the relevant literature. The error is small, which provides an important reference for the analysis of submarine hydrodynamic performance.

ACKNOWLEDGEMENTS

This work is supported by the National Natural Science Foundation of China (52131102), to which the authors are most grateful.

REFERENCES

Jeon, M, Mai, TL, Yoon, HK, Ryu, J, Lee, W, and Ku, P (2021). Evaluation of dynamic characteristics for a submerged body with large angle of attack motion via CFD analysis[J]. *Journal of Ocean Engineering and Technology*, 35(5): 313-326.

Lavrov, A, Rodrigues, JM, Gadelho, JFM, and Soares, CG (2017). Calculation of hydrodynamic coefficients of ship sections in roll motion using Navier-Stokes equations[J]. *Ocean engineering*, 133: 36-46.

Liang, X, Ma, N, Liu, H, and Gu, X (2021). Experimental study on the maneuvering derivatives of a half-scale SUBOFF model in the vertical plane[J]. *Ocean Engineering*, 233: 109052.

Lin, YH, Tseng, SH, and Chen, YH (2018). The experimental study on maneuvering derivatives of a submerged body SUBOFF by implementing the Planar Motion Mechanism tests[J]. *Ocean Engineering*, 170: 120-135.

Lin, YH, and Chiu, YC (2022). The estimation of hydrodynamic coefficients of an autonomous underwater vehicle by comparing a dynamic mesh model with a horizontal planar motion mechanism experiment[J]. Ocean Engineering, 249: 110847.

Mansoorzadeh, S, and Javanmard, E (2014). An investigation of free surface effects on drag and lift coefficients of an autonomous underwater vehicle (AUV) using computational and experimental fluid dynamics methods[J]. *Journal of Fluids and Structures*, 51: 161-171.

Pan, Y, Zhang, H, and Zhou, Q (2012). Numerical prediction of submarine hydrodynamic coefficients using CFD simulation[J]. *Journal of Hydrodynamics*, 24(6): 840-847.

Roddy, RF (1990). "Investigation of the Stability and Control Characteristics of Several Configurations of the DARPA Suboff Model (DTRC Model 5470) from Captive-Model Experiments."

Suzuki, H, Sakaguchi, J, Inoue, T, Watanabe, Y, and Yoshida, H (2013). Evaluation of methods to estimate hydrodynamic force coefficients of underwater vehicle based on CFD[J]. *IFAC Proceedings Volumes*, 46(33): 197-202.

Yang, LC, Pang, YJ, Huang, LH, and Zhang, AP (2009). Study of the CFD approach to simulate PMM experiments of submarines. *Ship Science and Technology*, 31(12): 12-17.

Yang, Y, Zou, ZJ, and Zhang, CX (2011). Calculation of hydrodynamic forces on a KVLCC hull in sway motion in deep and shallow water[J]. *Chinese journal of hydrodynamics*, 26(1): 85-93.